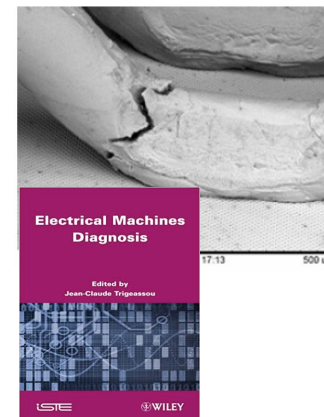
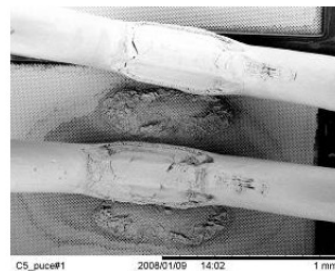
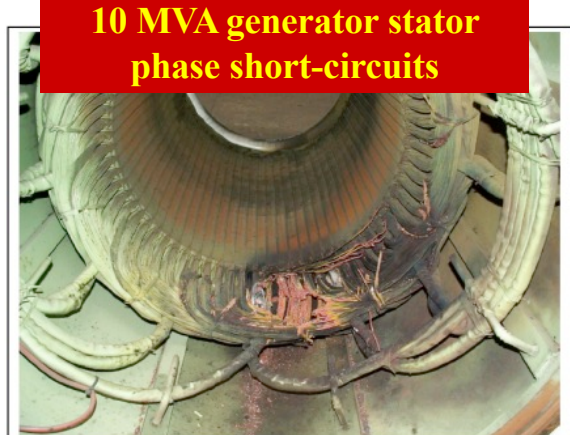


Fault Detection and Diagnosis Methodology & Applications

D. DIALLO

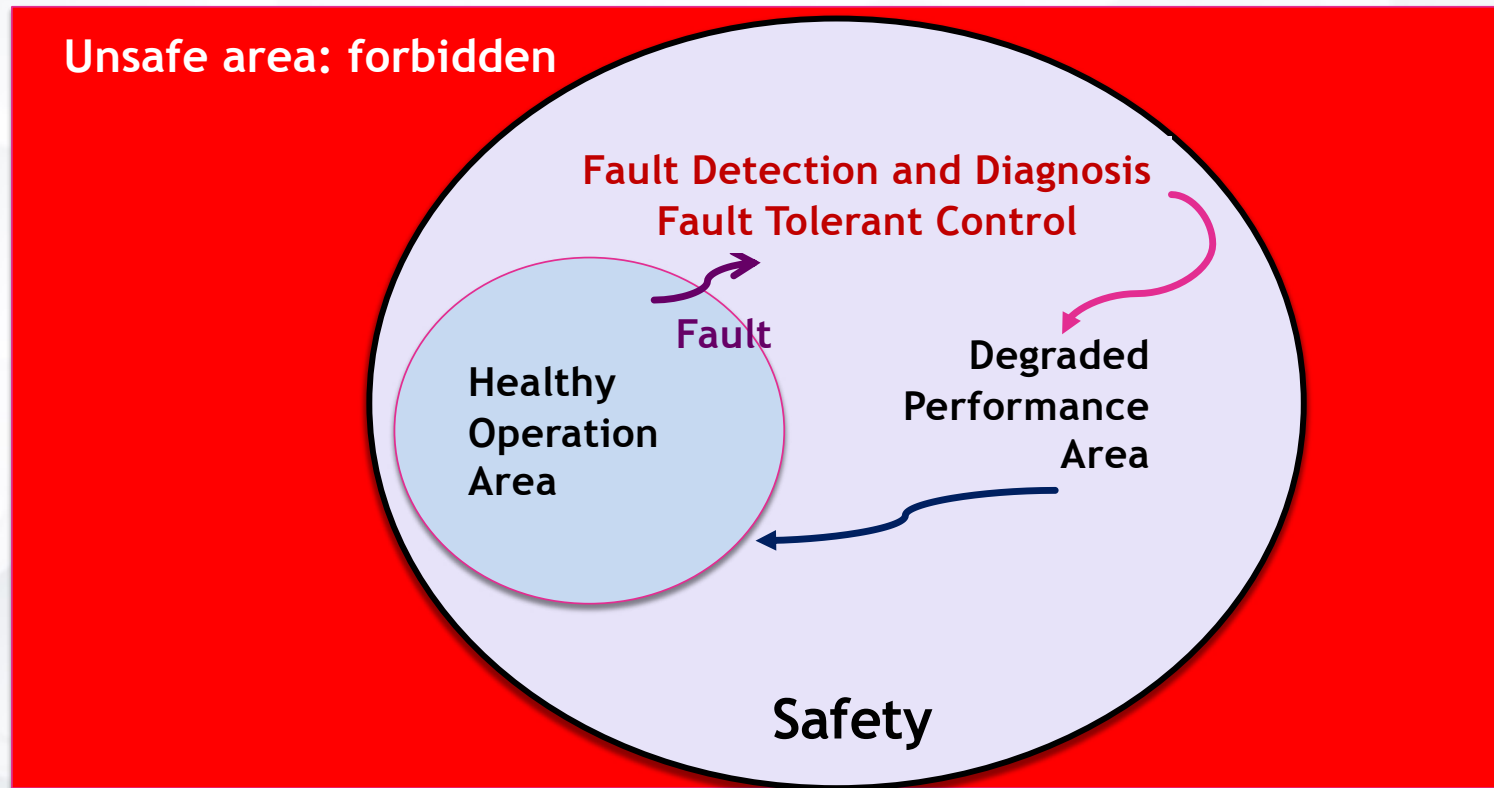
Université Paris-Saclay, CentraleSupélec, CNRS, Gif Sur Yvette, 91192, France



B. Brooks, "The bakersfield lesson in ground-fault protection,"
SolarPro Magazine, pp. 62-70, 2011.

1. Introduction to Fault Detection and Diagnosis

Safety and Fault Tolerance

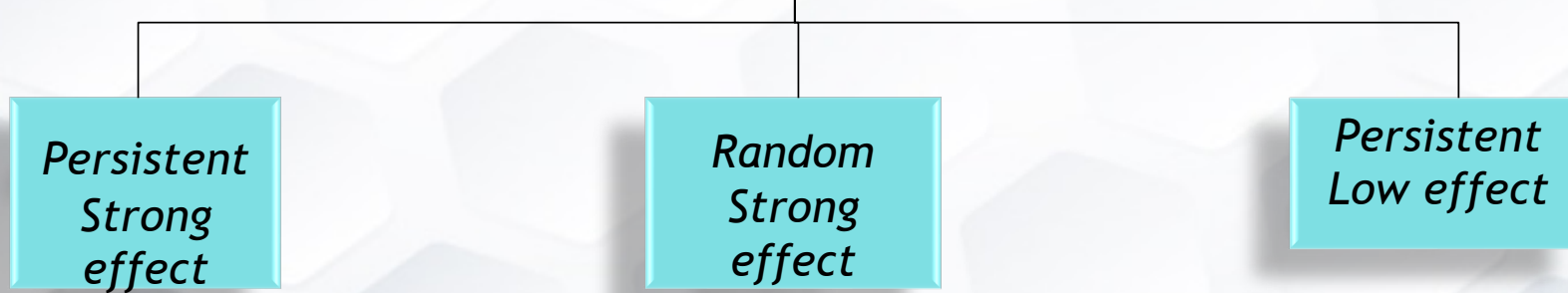


1. Introduction to Fault Detection and Diagnosis

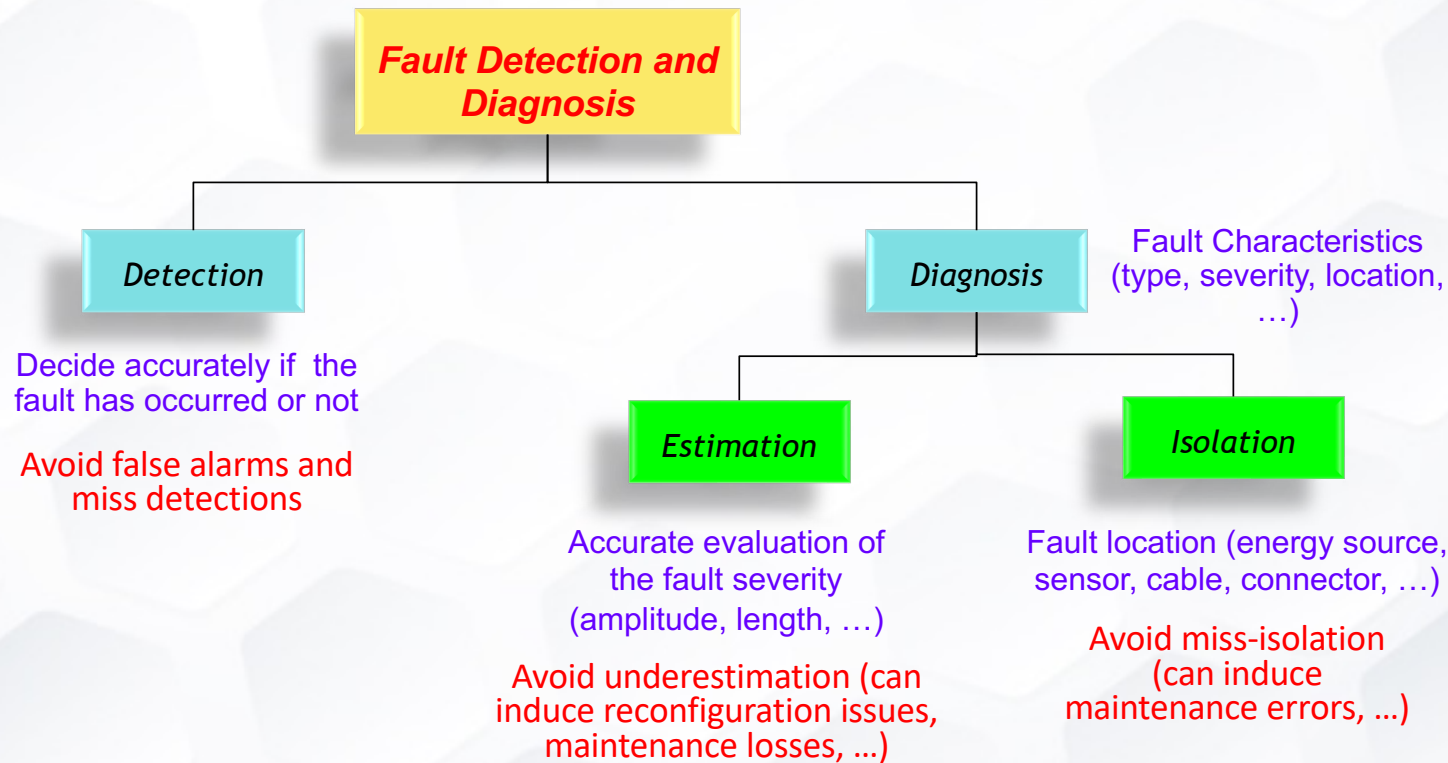
Fault types

A parameter or a variable is out of its 'healthy' operating range

Fault

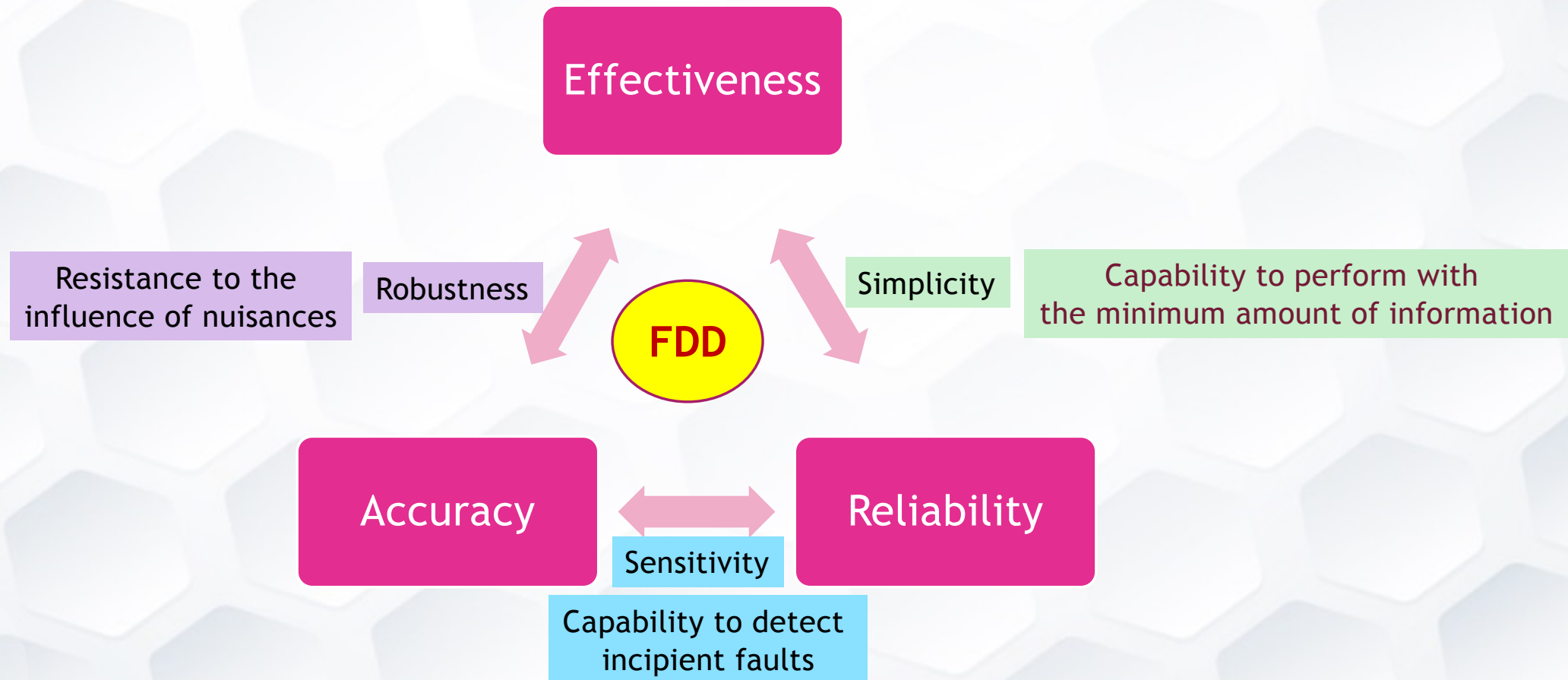


1. Introduction to Fault Detection and Diagnosis



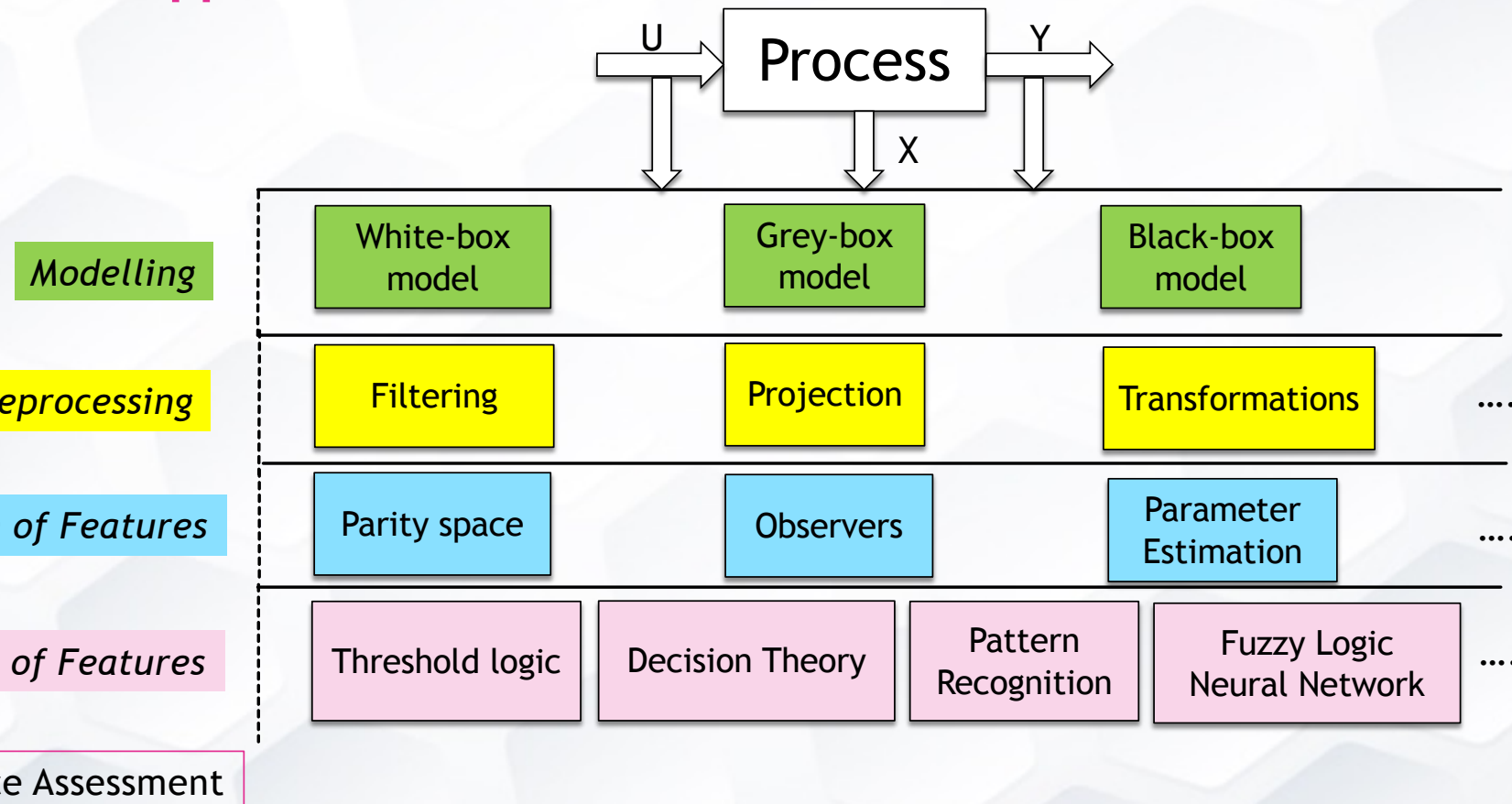
1. Introduction to Fault Detection and Diagnosis

Fault Detection and Diagnosis Methods: A compromise



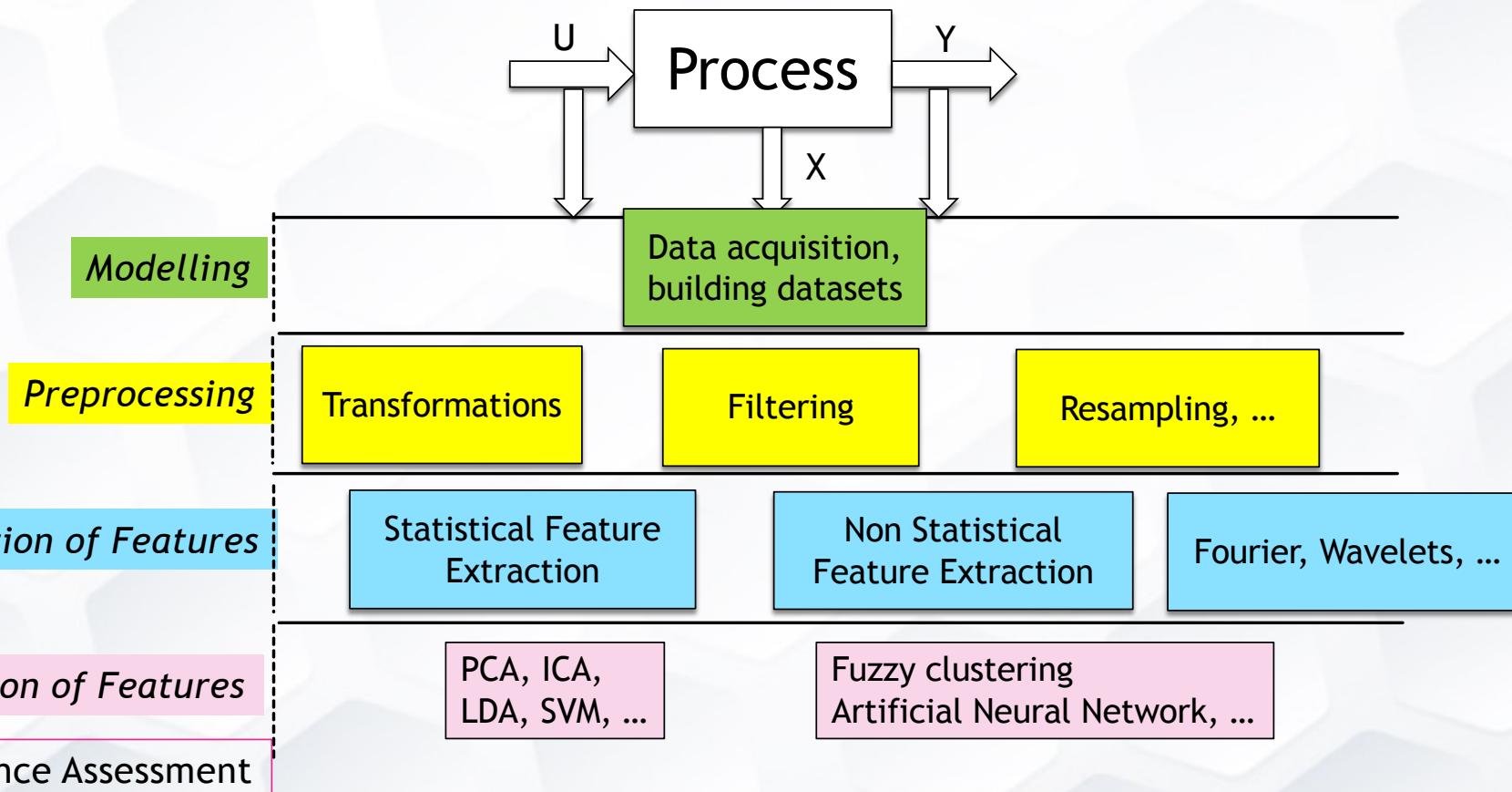
1. Introduction to Fault Detection and Diagnosis

Physics-based approach: General Scheme



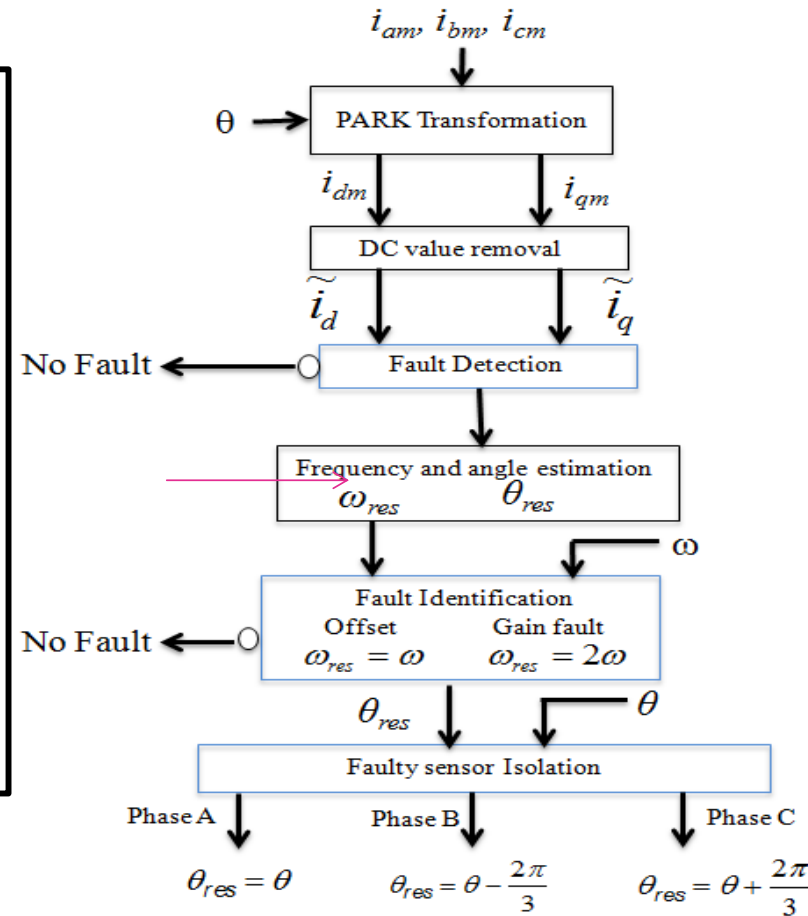
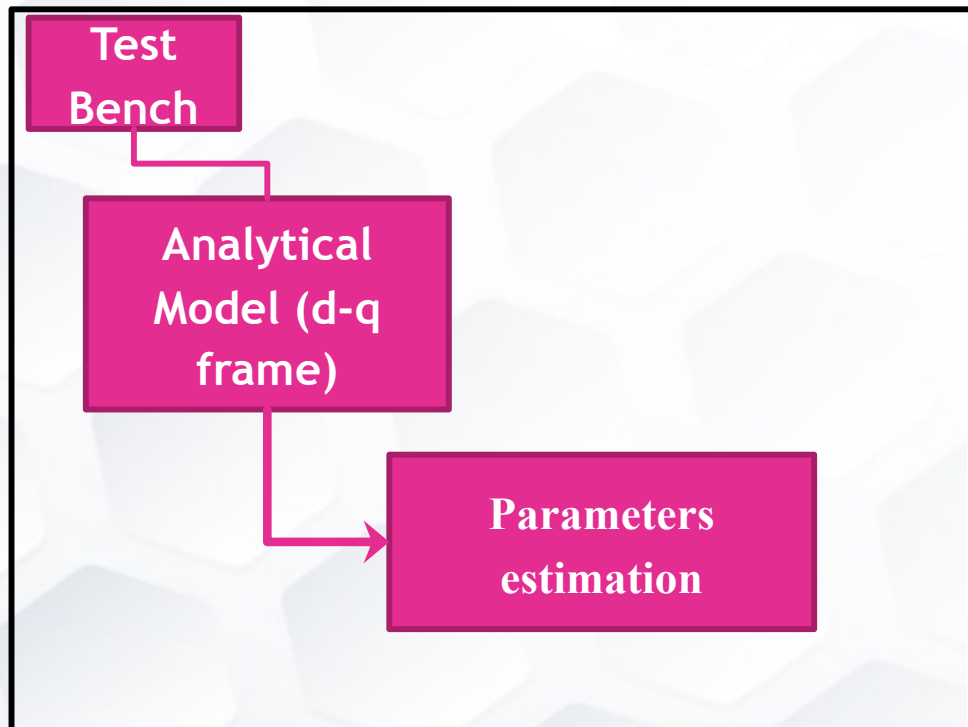
1. Introduction to Fault Detection and Diagnosis

Data-driven approach: General Scheme



2. Applications

Phase Current Sensors Fault Diagnosis: Physics-based, Estimation in the Park reference frame

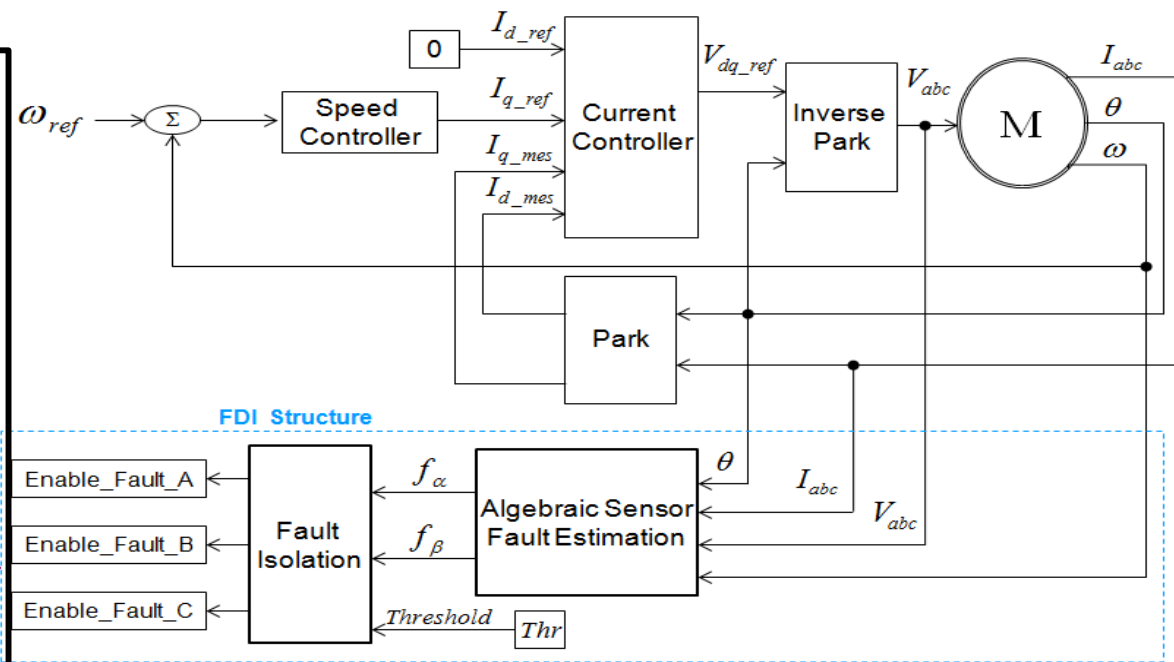
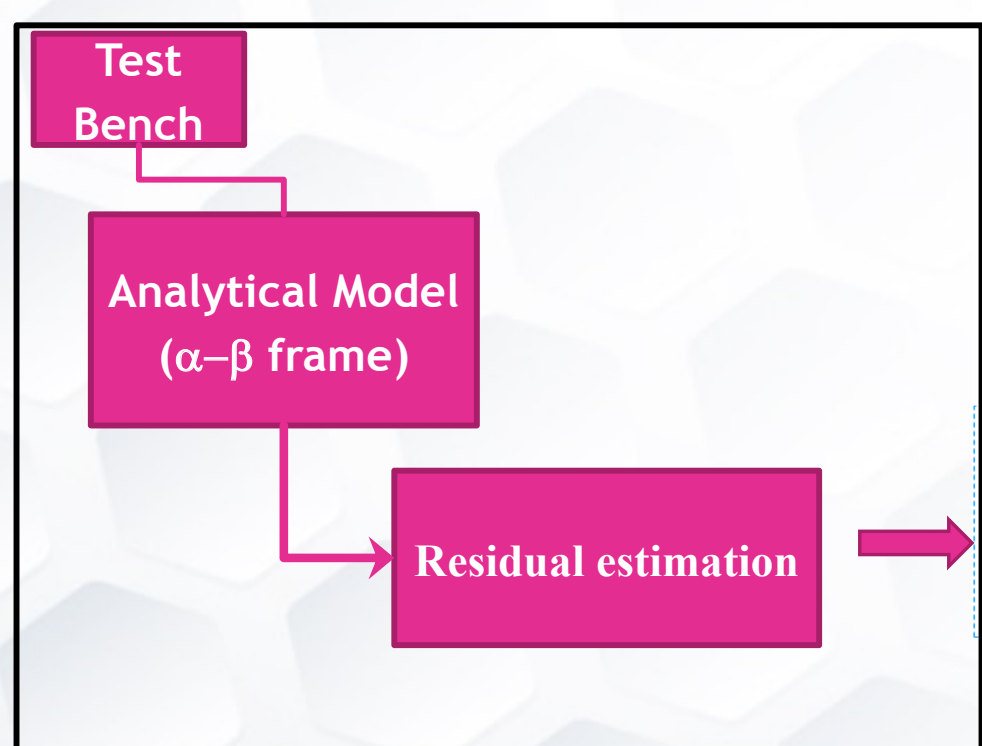


$$\theta_{res} = \arctan\left(-\frac{\tilde{i}_d}{\tilde{i}_q}\right),$$

$$\omega_{res} = \frac{d}{dt} \theta_{res}$$

2. Applications

Phase Current Sensors Fault Diagnosis: Physics-based, Estimation in the Concordia reference frame



$|f_\alpha| > thr$ and $|f_\beta| < thr \Rightarrow$ phase A sensor is faulty

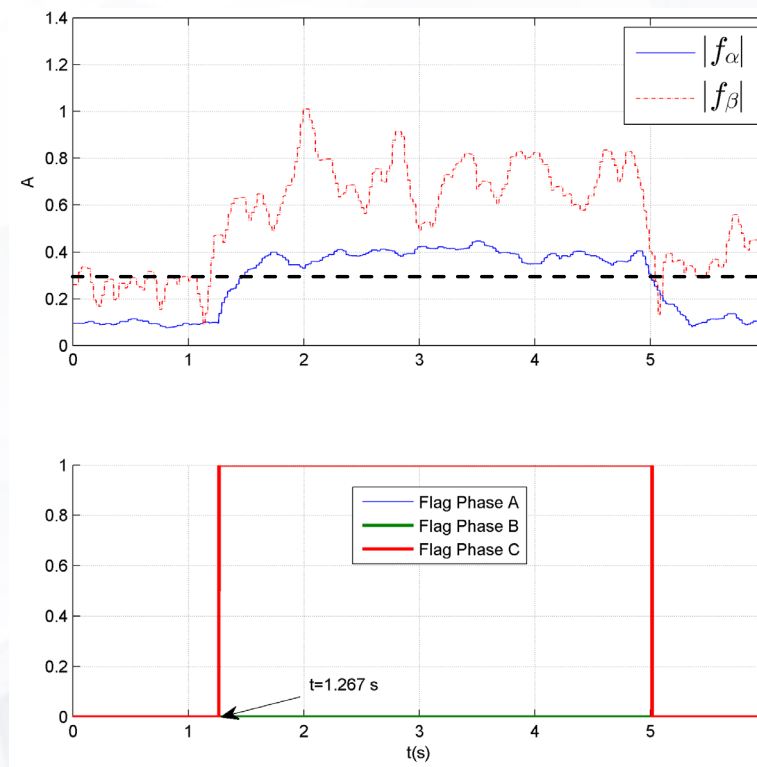
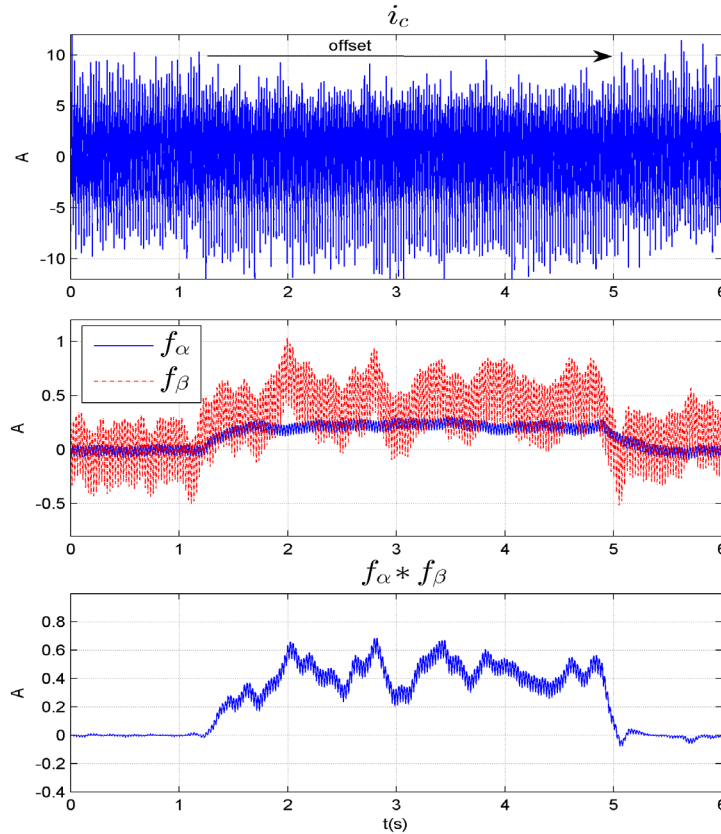
$f_\alpha > thr$ and $f_\beta > thr$ and $f_\beta * f_\alpha < 0 \Rightarrow$ phase B sensor is faulty

$f_\alpha > thr$ and $f_\beta > thr$ and $f_\beta * f_\alpha > 0 \Rightarrow$ phase C sensor is faulty

2. Applications

Phase Current Sensors Fault Diagnosis

Experimental results (offset in phase C of 16% on the peak value)



$$|r_\alpha| = 0.42$$

$$|r_\beta| = 0.707$$

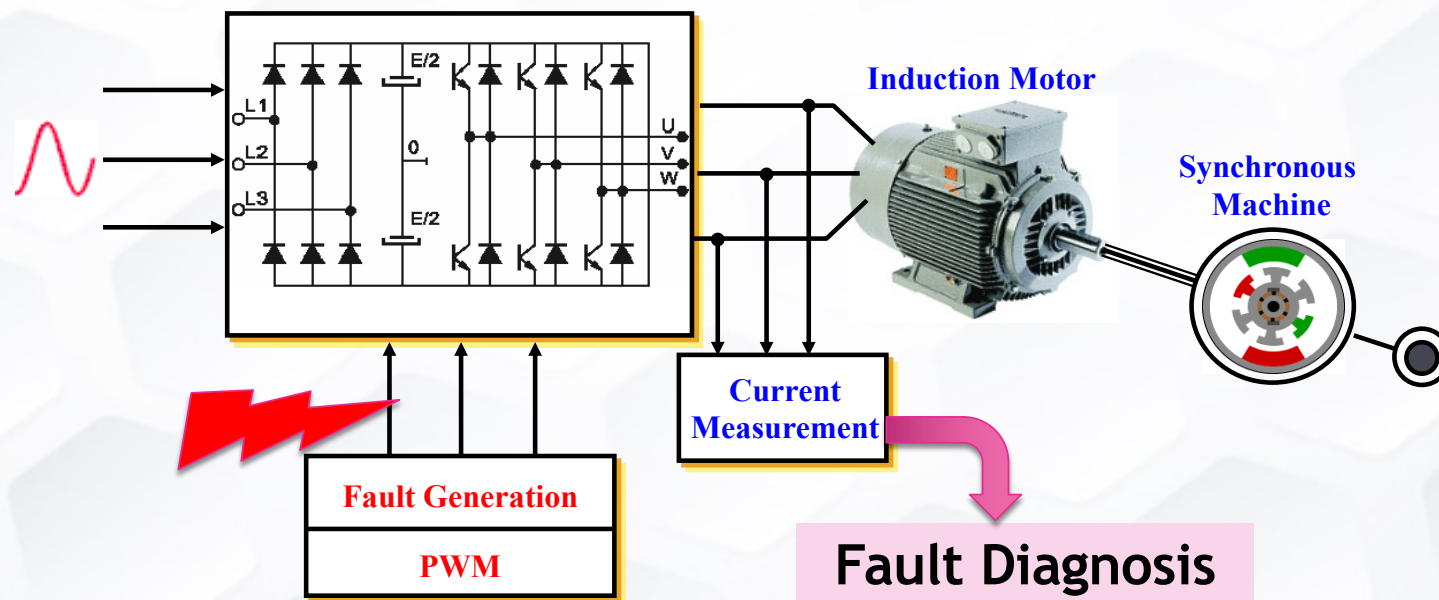
$$|\hat{r}_\alpha| = 0.4$$

$$|\hat{r}_\beta| = 0.72$$

2. Applications

Power converter misfiring fault diagnosis

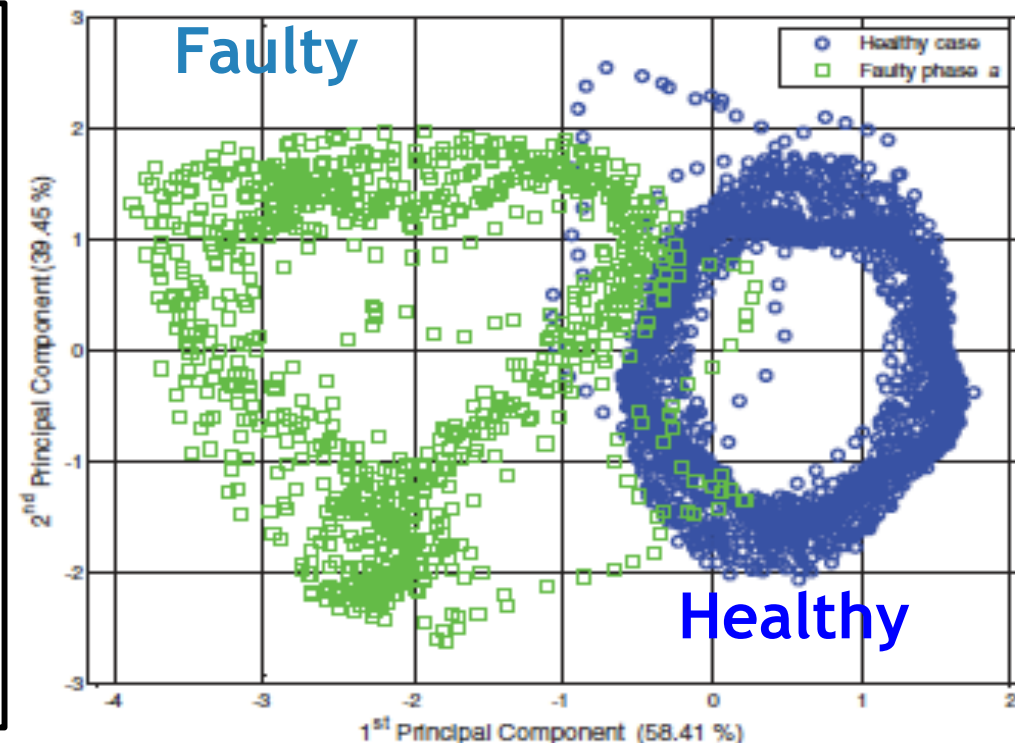
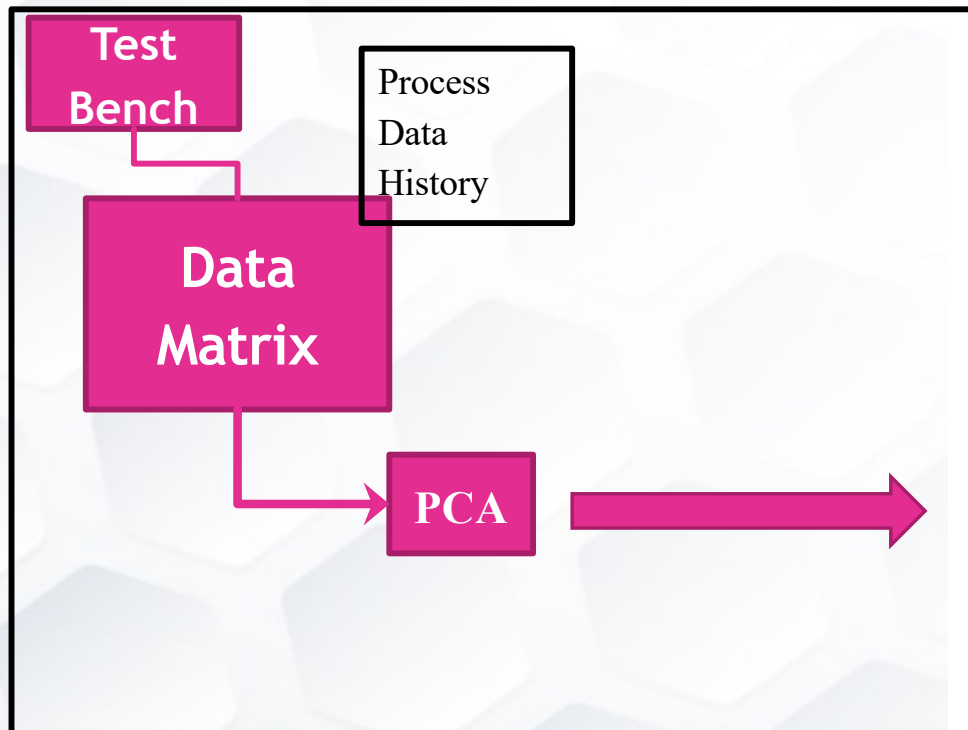
- 0.3 kW Induction Motor 0.3kW, 230/400V, 1.47/0.85 A, 1380 rpm



- Sampling and switching period 1ms

2. Applications

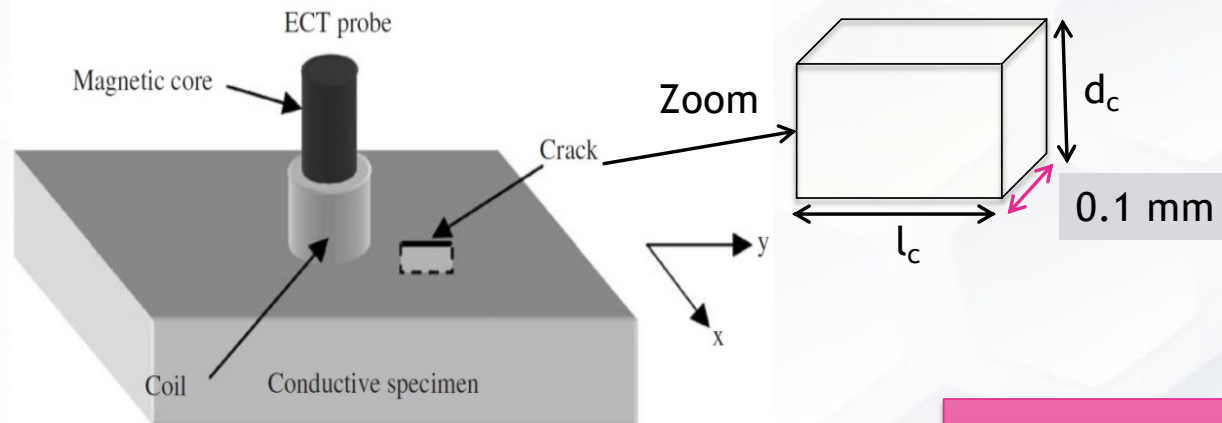
Power converter misfiring fault diagnosis: Data-based classification



Classification in PCA framework

2. Applications

Application to Non-Destructive Evaluation with Eddy Current



Electric discharge machining thin cracks into a nickel-base plate
Crack dimensions :

Small Cracks

Area (mm ²)	0.01 0.02	0.04 0.06	0.08 0.12	0.16 0.24
l_c, d_c (mm)	0.1, 0.1 0.1, 0.2	0.1, 0.4 0.6, 0.1	0.2, 0.4 0.6, 0.2	0.4, 0.4 0.6, 0.4

2. Applications

Application to Non-Destructive Evaluation with Eddy Current

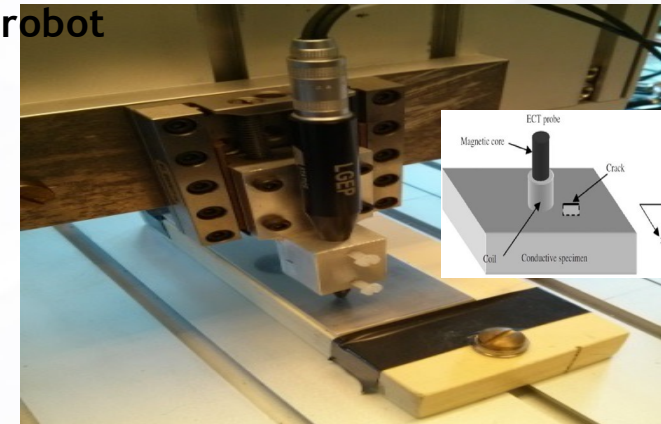
Experimental test bed [1]

Agilent 4294A Precision Impedance Analyser



$$f_{exc} = \{0.1, 1, 1.5, 3, 4, 5, 6\} \text{ MHz}$$

A three-axis computer-controlled robot



$$Z_d = R_d + j2\pi f_{exc} L_d \quad (\Delta x, \Delta y) = (0.1; 0.1) \text{ mm}$$

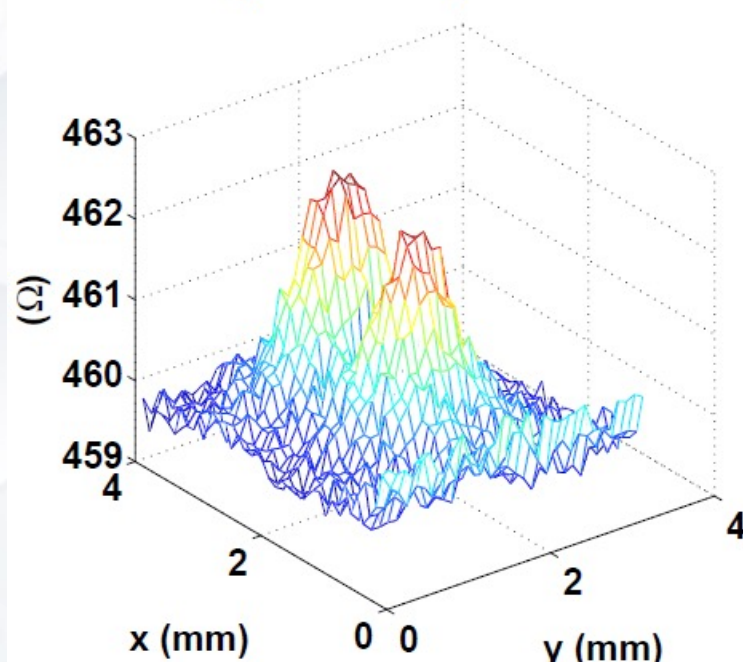
The Imaginary part is the most affected and will be under study

[1] Y. L. Bihan, J. Pavo, and C. Marchand, "Characterization of small cracks in eddy current testing", *The European Physical Journal Applied Physics*, vol. 43, no. 2, pp. 231–237, 2008.

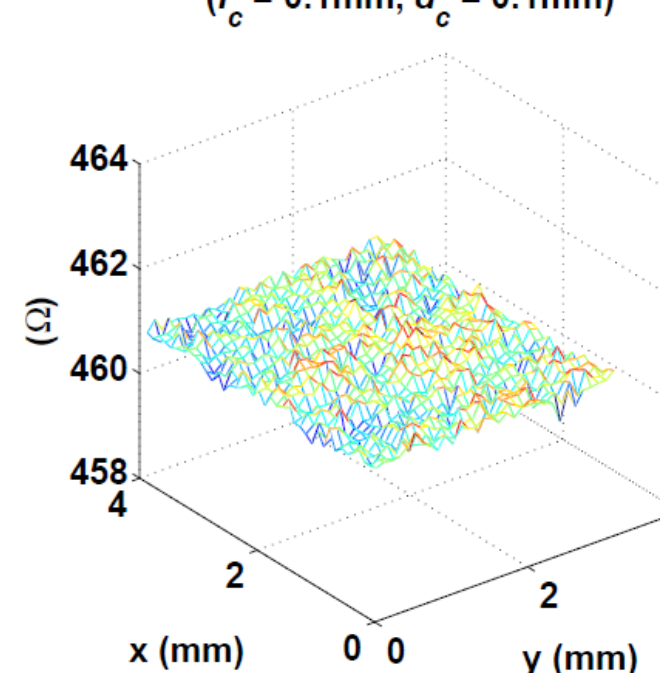
2. Applications

Application to Non-Destructive Evaluation with Eddy Current

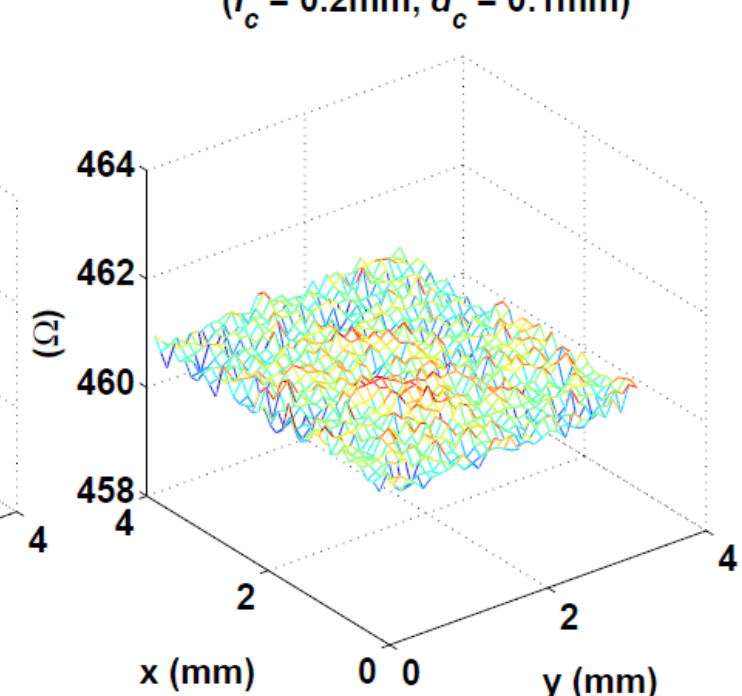
$(I_c = 0.4\text{mm}, d_c = 0.6\text{mm})$



$(I_c = 0.1\text{mm}, d_c = 0.1\text{mm})$

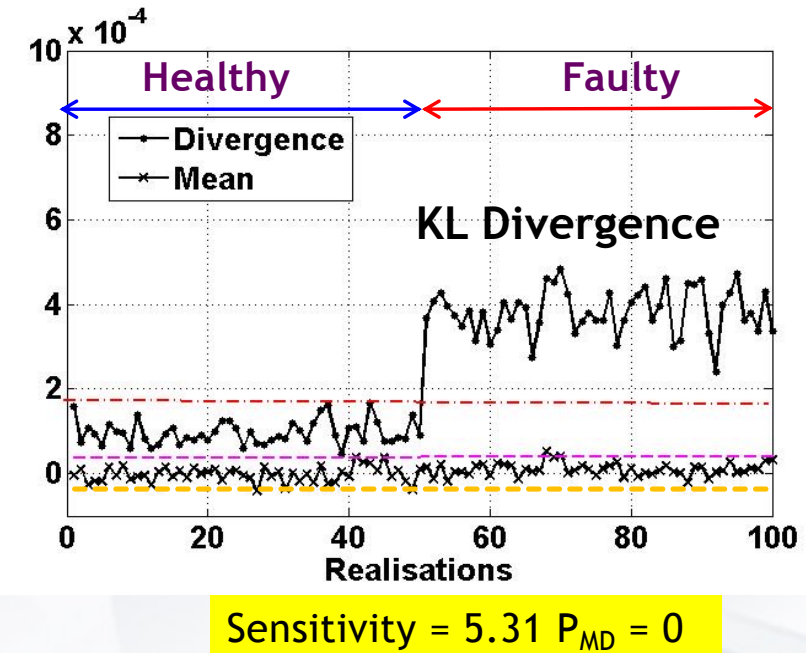
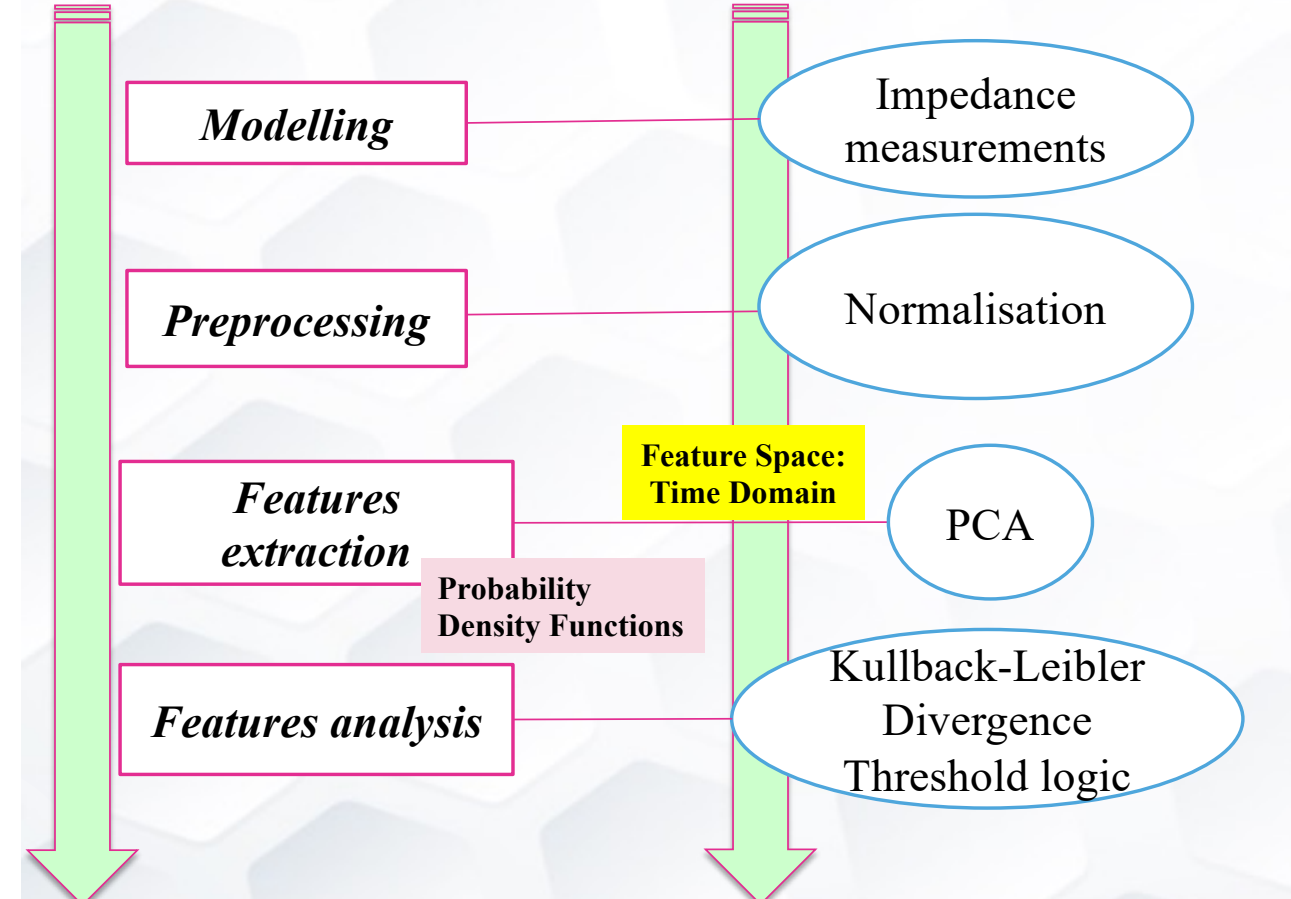


$(I_c = 0.2\text{mm}, d_c = 0.1\text{mm})$



2. Applications

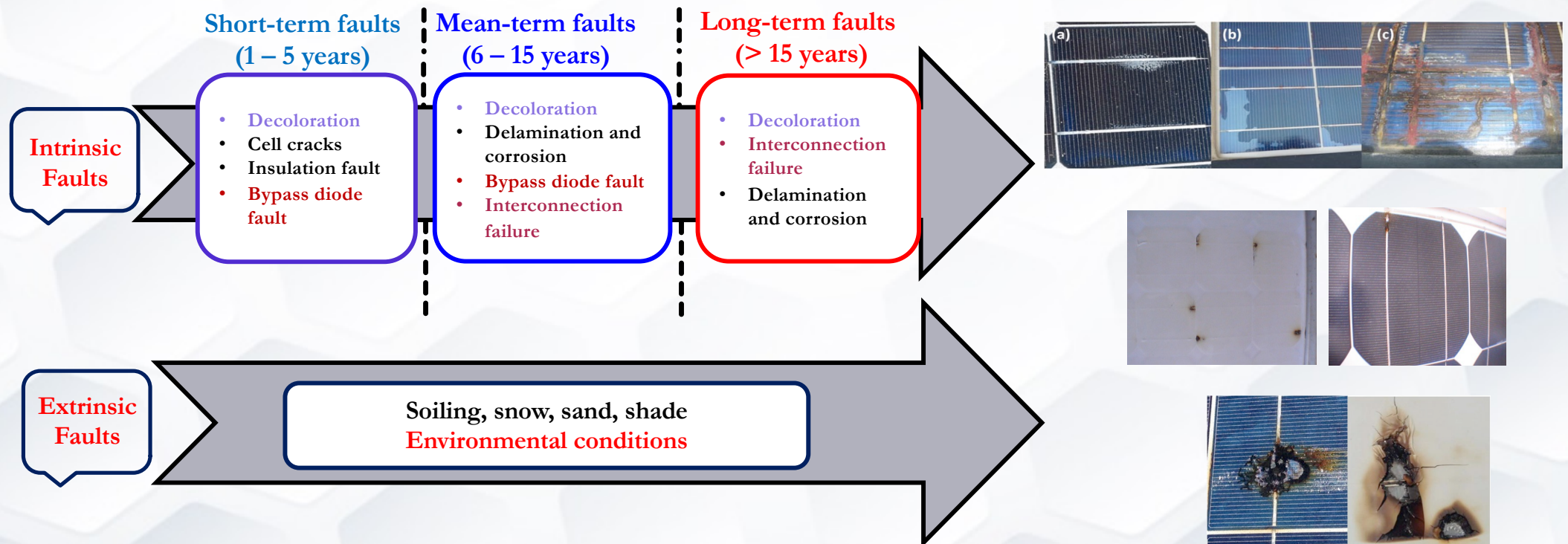
Application to Non-Destructive Evaluation with Eddy Current: Data-driven approach



2. Applications

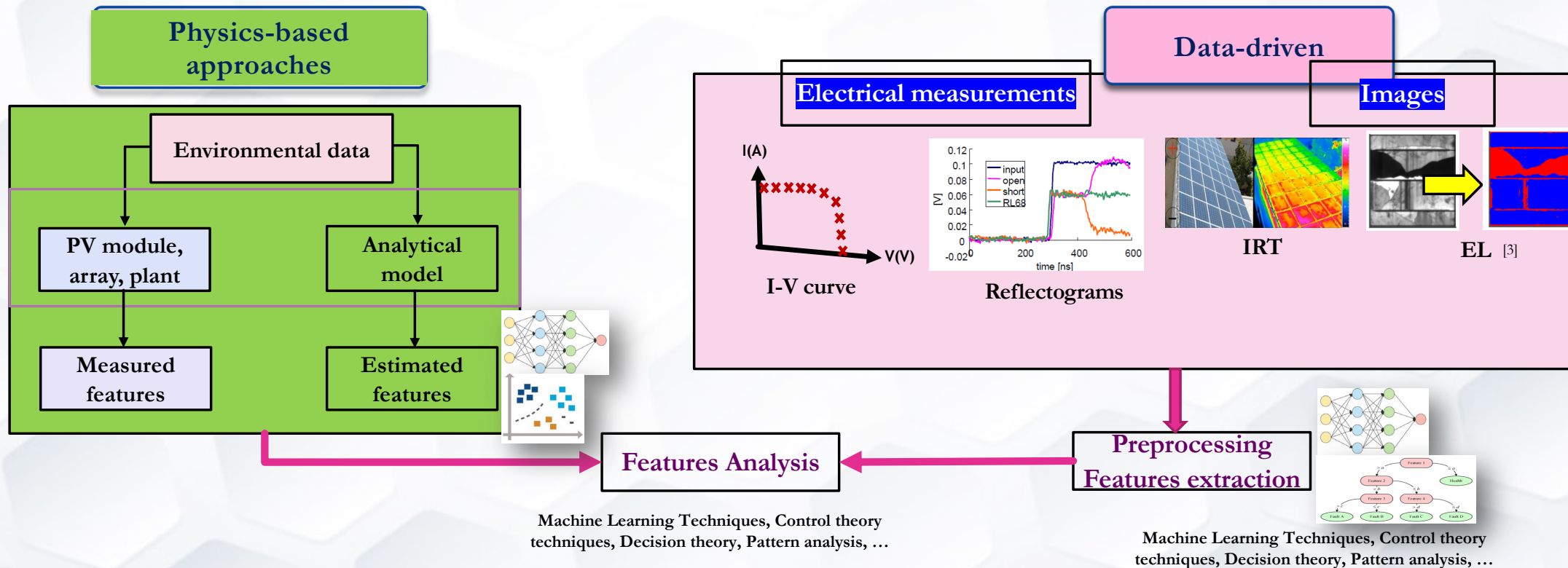
Application to PV module fault diagnosis

Timelines of the main defects of PV cells and modules



2. Applications

Application to PV module fault diagnosis



[3] S. Spataru. Characterization and Diagnostics for Photovoltaic Modules and Arrays, Department of Energy Technology, Aalborg University, 2015. 141 p. Research output: Book/Report > Ph.D. thesis

2. Application to PV modules

□ Fault diagnosis using I-V curves

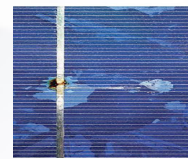
Modeling Pre-process Feature extraction Feature analysis

Fault effects on the I-V curves

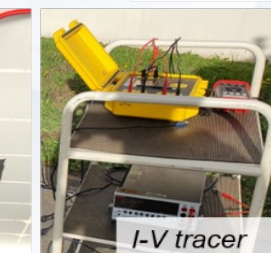
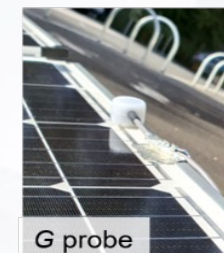
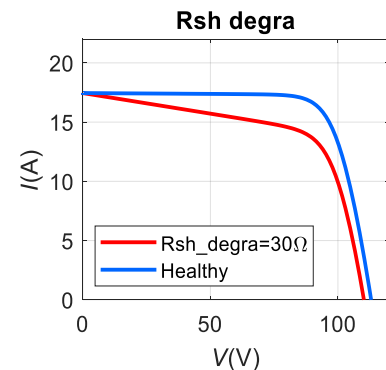
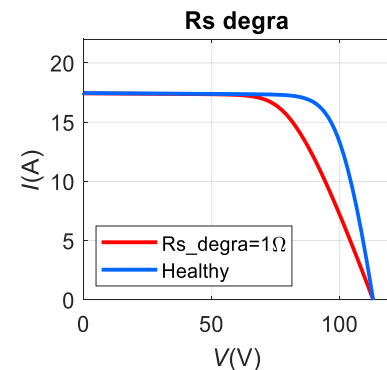
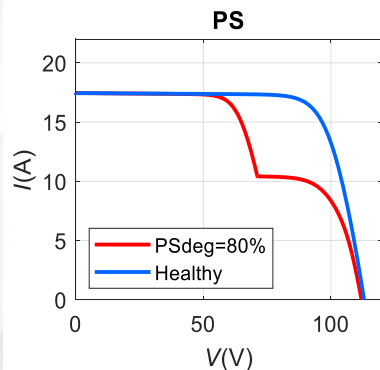
Partial Shading



Degradation of the contacts



Delamination



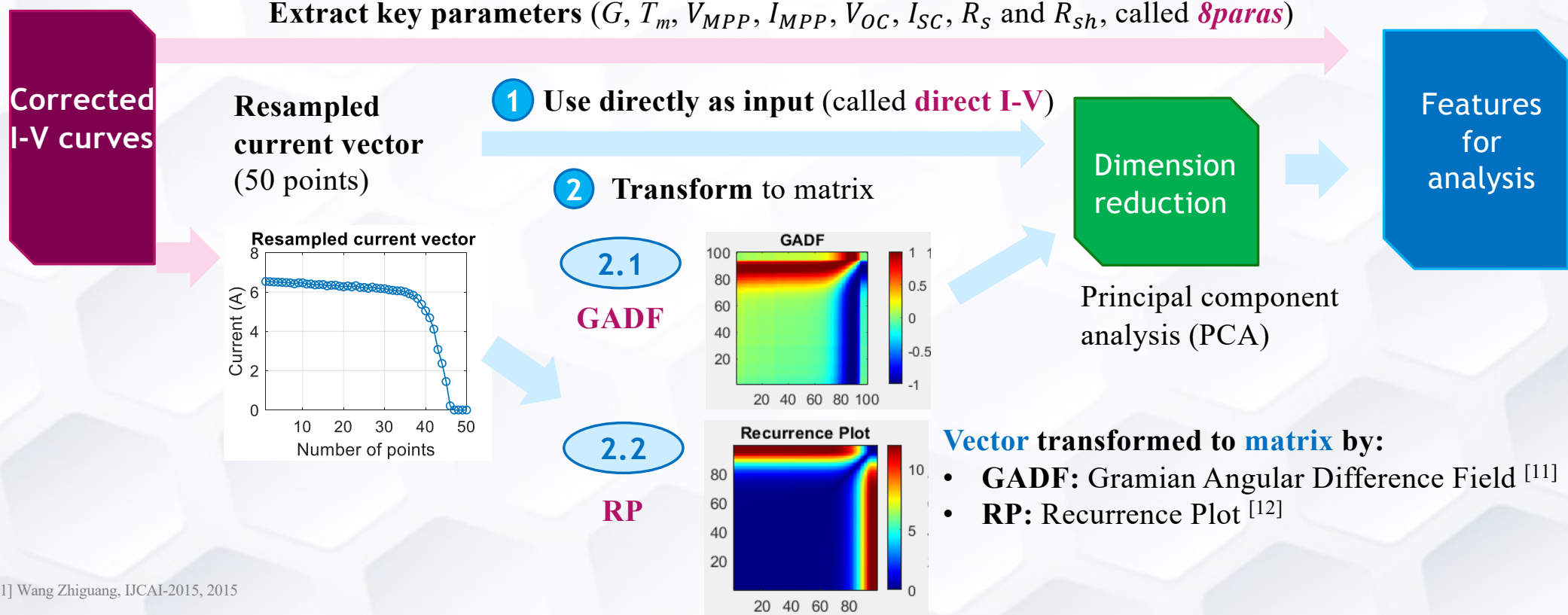
(Reference cell RG100)
(Pt100)

(FTV200)

2. Application to PV modules

□ Feature extraction from I-V curve

Modeling Pre-process **Feature extraction** Feature analysis

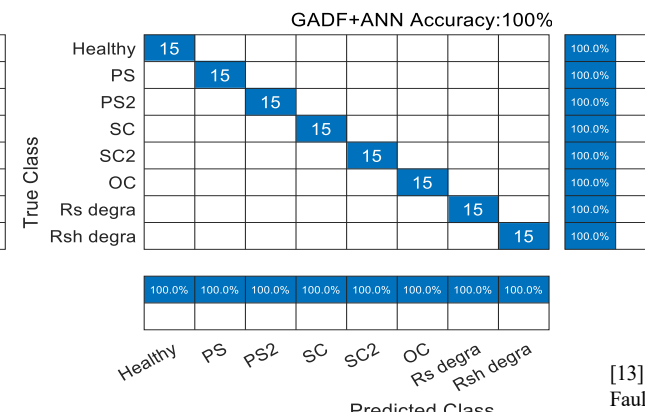
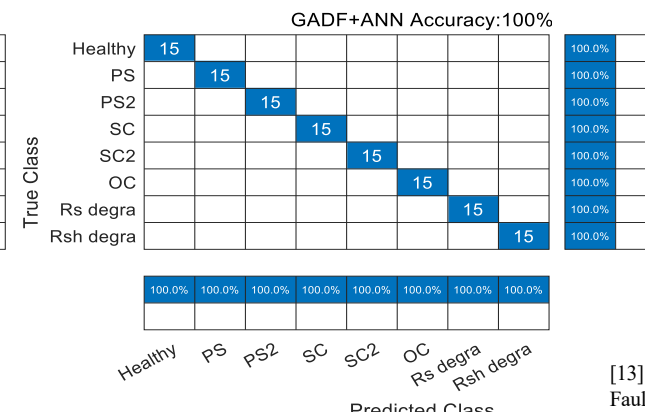
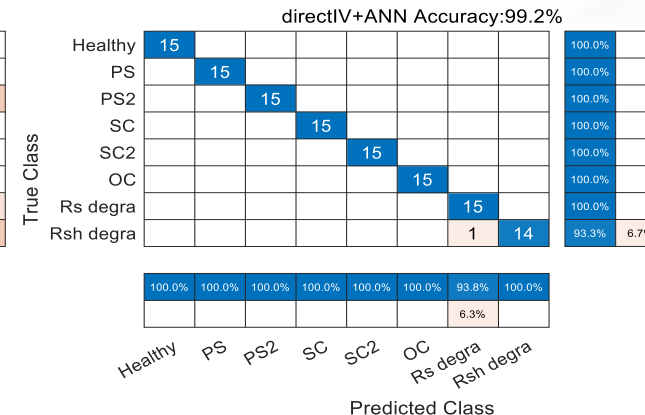
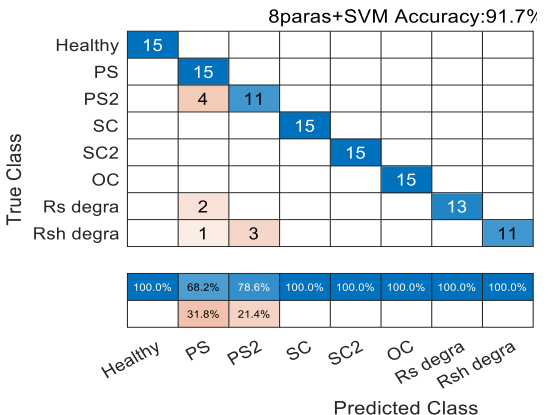


[11] Wang Zhiguang, IJCAI-2015, 2015

[12] Marwan N, Physics reports, 2007, 438(5-6): 237-329

2. Application to PV modules

□ Test results using field-measured data [13]



Modeling Pre-process Feature extraction Feature analysis

ANN

Artificial Neural Network

SVM

Support Vector Machine

NBC

Naive Bayes Classifier

DT

Decision Tree

RF

Random Forest

kNN

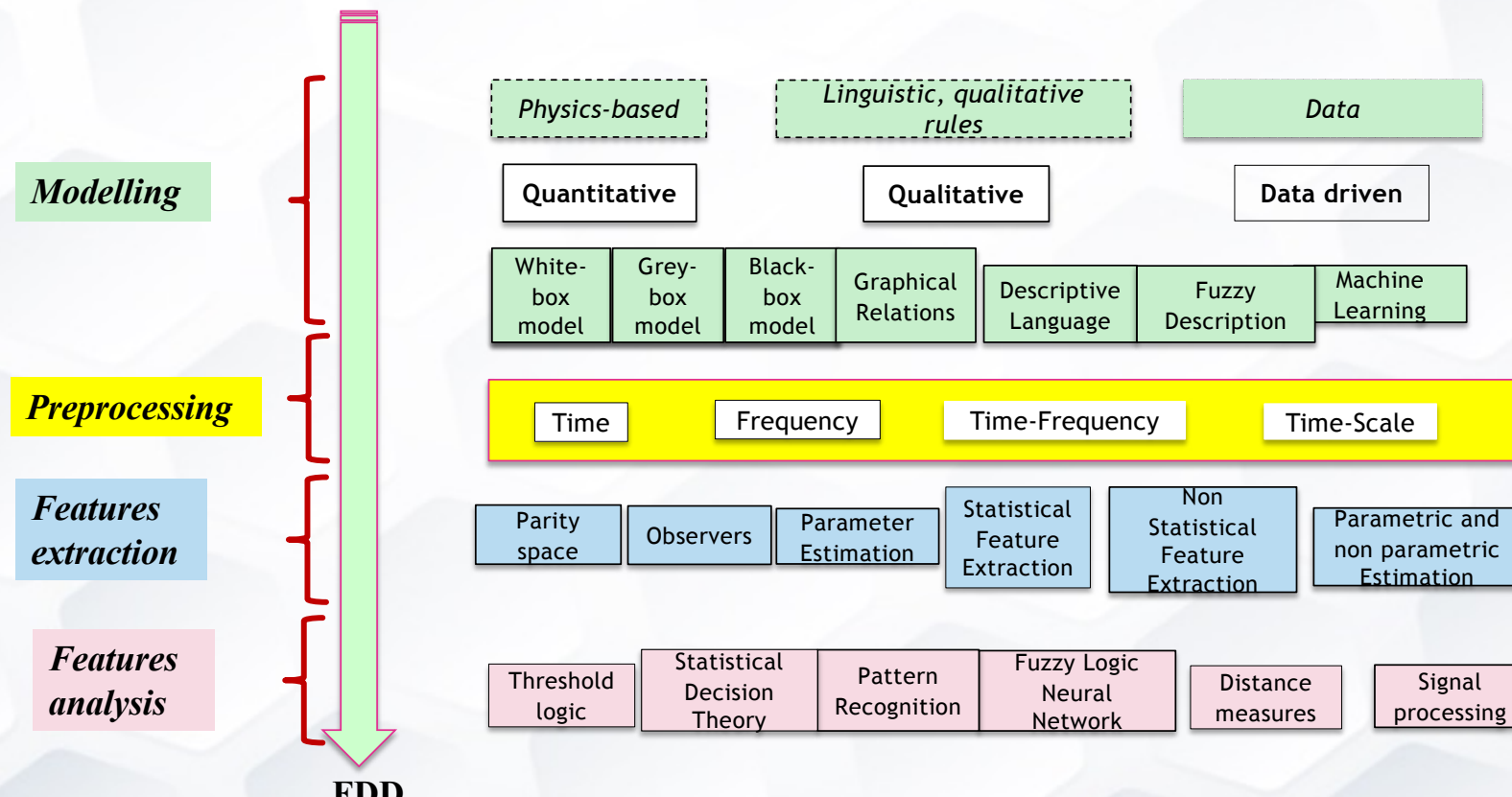
k-Nearest Neighbors

[13] Li B., Delpha C., Migan A., Diallo D.

Fault Diagnosis of Photovoltaic Panels Using Full I-V Characteristics and Machine Learning Techniques.
Energy Conversion and Management 248 (2021). doi: 10.1016/j.enconman.2021.114785

3. Conclusion

In summary: a 4-step FDD methodology



[1] Delpha, C.; Diallo, D. Kullback–Leibler divergence for incipient fault diagnosis. In Signal Processing for Fault Detection and Diagnosis in Electric Machines and Systems; Benbouzid, M., Ed.; IET, The Institution of Engineering and Technology, 2020

Thank you!



université
PARIS-SACLAY

demba.diallo@universite-paris-saclay.fr